Original paper

Mechanism of pruritus ani lotion combined with Huajiao-Gancao-Bingpian oil for pruritus ani treatment based on network pharmacology and molecular dynamics

Wenkuo Deng, Minghong Fu, Jintao Huang

Anorectal Department, Xiangyang Hospital of Traditional Chinese Medicine [Xiangyang Institute of Traditional Chinese Medicine], Xiangyang City, Hubei Province, China

Adv Dermatol Allergol 2024; XLI (2): 203–214
DOI: https://doi.org/10.5114/ada.2023.135761

Abstract

Introduction: Pruritus ani lotion combined with a Chinese medicine formula named Huajiao (Pericarpium Zanthoxyli Bungeani)-Gancao (Radix Glycyrrhizae)-Bingpian (Borneol) is effective in treating pruritus ani.

Aim: To investigate the mechanism of traditional Chinese medicine (TCM) in pruritus ani via network pharmacology and molecular dynamics (MD).

Material and methods: The Traditional Chinese Medicine Systems Pharmacology Database and Analysis Platform (TCMSP) was utilised to screen active ingredients and their corresponding targets. Genes associated with pruritus ani were collected through GeneCards. Protein-protein interaction (PPI) network between target genes of the active ingredients of this formula and genes associated with pruritus ani was established through the STRING database. A drug-active ingredient-gene interaction network was constructed using Cytoscape with the top 50 genes in affinity coefficients. Molecular docking and MD simulation analysis were performed.

Results: Epidermal growth factor receptor (EGFR) and Signal Transducer and Activator of Transcription 3 (STAT3) were core genes. Direct targeting of EGFR by the active ingredients (quercetin and luteolin) and direct targeting of STAT3 by the active ingredient (licochalcone A) may be key molecular mechanisms for the treatment of pruritus ani. Simulated trajectories of structural nuclear motion by MD also revealed that the binding of two pairs of molecules was relatively stable.

Conclusions: This study unravels potential targets, active ingredients, and mechanisms of pruritus ani lotion combined with Huajiao-Gancao-Bingpian oil in the treatment of pruritus ani, providing a reference for future treatment.

Key words: pruritus ani lotion, Huajiao-Gancao-Bingpian oil, pruritus ani, network pharmacology, molecular dynamics.

Introduction

Pruritus ani includes diseases like anal pruritus and anal eczema. Anal eczema is a non-infectious inflammatory disease of the anal skin that is primarily distinguished by itching, erosion, and rash on the perianal area. The primary cause of pruritus ani could be a combination of irritants such as faecal contamination and dietary factors, but secondary causes are also possible, including malignancy, infection (including sexually transmitted diseases), benign anorectal disease, systemic disease, and inflammatory disease [1]. At present, pruritus ani is mainly treated by conservative non-drug perianal hygiene care. The therapy involves the use of local medications, such as local steroids, antibacterial, antifungal, anaesthetics, and analgesics. The therapeutic benefits of astringents such as ephedrine and vasoconstrictors in the treatment of pruritus ani are limited [2]. Recurrent pruritus ani continues to have an impact on the patients' physical and mental health, as well as their quality of life, throughout the course of therapy. Also, it tends to recur after cure [3]. Hence, there is a pressing need for better treatment that also comes with improved outcomes of pruritus ani.

Traditional Chinese medicine (TCM) believes that the aetiology of pruritus ani is mostly damp-heat, endogenous wind, blood deficiency, and sometimes worm infection. Excessive cleaning easily damages the skin [4]. TCM has a substantial impact on pruritus ani treatment. Sitz bath is one of the main clinical treatments for anal pruritus. Simple anal pruritus symptoms can be adequately treated with a shenbai decoction sitz bath [4]. For pruritic skin condi-

Address for correspondence: Jintao Huang, Anorectal Department, Xiangyang Hospital of Traditional Chinese Medicine [Xiangyang Institute of Traditional Chinese Medicine], 112 Changzheng road, Fancheng area, Xiangyang City, Hubei Province, 441000, China, phone: +86 13972222340, e-mail: 17560575@qq.com
Received: 22.08.2023, **accepted:** 10.10.2023, **online publication:** 25.04.2024.

tions, acupuncture may be beneficial. Guo *et al*. discovered that self-made Chinese herbal fumigant combined with acupuncture at Dong's extra acupoints significantly improve the clinical symptoms of patients with pruritus ani. Moxibustion treatment can reduce the degree of pruritus and frequency of pruritus and increase the life quality of patients with pruritus ani. Smoking moxibustion has a more beneficial therapeutic effect than smokeless moxibustion since the main products of moxa smog are what give it its antipruritic impact [5]. In conclusion, TCM is effective in treating pruritus ani. We will thus continue to investigate the molecular basis of TCM therapies for pruritus ani.

We previously found that the pruritus ani lotion sitz bath combined with a Chinese medicine formula named Huajiao (Pericarpium Zanthoxyli Bungeani)-Gancao (Radix Glycyrrhizae)-Bingpian (Borneol) oil first mentioned in *Zhao Bingnan's Clinical Experience Collection* had a significant effect on pruritus ani, but the underlying mechanism remained elusive. Network pharmacology was utilised to analyse the active ingredients of pruritus ani lotion and Huajiao-Gancao-Bingpian oil, combined with protein-protein interaction (PPI) network and random walk with restart (RWR) method to analyse its key genes and signalling pathways in the treatment of pruritus ani. Further molecular dynamics (MD) simulation verified the docking relationship between active ingredients and target genes to explore the potential mechanism of pruritus ani lotion combined with Huajiao-Gancao-Bingpian oil for external use, providing a theoretical framework for the management of pruritus ani.

Material and methods

Collecting active ingredients and targets of drugs and pruritus ani-related genes

In TCM Systems Pharmacology Database and Analysis Platform (TCMSP) (https://tcmsp-e.com/), the chemical composition of pruritus ani lotion (Cnidium monnieri, Kochia scoparia, Cortex Phellodendron, Radix Sophorae Flavescentis, Radix Baibu, Radix Angelicae Sinensis, Clematis, Pericarpium Zanthoxyli Bungeani, Cortex Phellodendri, Portulaca oleracea, Alum, Glauber's salt) and Huajiao-Gancao-Bingpian oil (sesame oil, Pericarpium Zanthoxyli Bungeani, Radix Glycyrrhizae, Borneol) were searched. Active ingredients with oral bioavailability (OB) ≥ 30% and drug-likeness (DL) ≥ 0.18 were selected. Besides, the information on targets corresponding to screened compounds was searched on TCMSP.

In GeneCards, we searched for genes associated with pruritus ani with the keyword Anal Itching. Ranked by relevance score, the top 100 genes were selected for subsequent studies.

Construction of a PPI network

Combined target genes and disease-associated genes, PPI analysis was performed through STRING (https://string-db.org/). A PPI network was then built with genes with interaction confidence scores greater than 0.7. RWR analysis was conducted on the PPI network obtained in the previous step with dnet package [6]. The intersection of target genes and disease-associated genes was used as seed. With a restart probability of 0.85, the adjacency matrix of the network graph was normalized using the Laplacian. RWR analysis was employed to determine the affinity coefficient between each gene and seed. The top 50 nodes with the highest affinity coefficients were chosen as the top 50 genes for further study. Cytoscape software was used to analyse the interaction between the formula, small active ingredient molecules, as well as the top 50 genes to build a formula-active ingredient-target gene interaction network.

Enrichment analyses

Gene ontology (GO) and Kyoto Encyclopedia of Genes and Genomes (KEGG) enrichment analyses (p-value < 0.05) of the top 50 genes were performed with the clusterProfiler package [7]. Combined with findings in other studies, the role of pathways was determined.

Molecular docking

NetworkX, a Python package, was utilised to analyse the topological features of the network. Node genes were ranked according to degree values, and key genes were selected for further analysis. With the PDB structure of target proteins from the PDB database (https://www.rcsb.org/), excess structures, ligands, and surrounding water molecules were deleted with PyMOL. Hydrogen atoms were added with AutoDock Tools software and the results were converted to pdbqt files. Subsequently, ProteinsPlus (https://proteins.plus/) was employed to predict pockets on protein structures while setting box-sizing and central coordinates. In PubChem database (https://pubchem.ncbi.nlm.nih.gov/), sdf files of active small molecules were converted to pdbqt files with AutoDock Tools software. Finally, AutoDock Vina software was utilised to simulate docking between pockets of protein structure and active small molecules. 3D and 2D plots of interactions between small molecules and surrounding residues were processed with Pymol software and Ligplot software, respectively.

MD simulation

After scoring the binding free energy of protein-small molecule docking, the protein-small molecule complex with the highest binding free energy was chosen. MD simulation was conducted with Gromacs (version 2021.3) software to investigate the intrinsic kinetic properties of small molecule binding proteins. CGenFF service (https://cgenff.umaryland.edu/) developed protein structure topology files utilising the CHARMM36 force field and TIP3P water model to produce topology and parameter files for

small molecules. To create a topology file for the protein-small molecule complex, the protein-small molecule complex was enclosed in a dodecahedron box with a border distance of 1.2. Ions with the same number of charges as in protein-small molecule complexes were added to neutralize the charge. Energy minimization was done by steep method with 50,000 steps followed by 100 ps of constant number, volume, and temperature (NVT) equilibration followed by 100 ps of constant number (N), pressure, and temperature (NPT) equilibration. The system was maintained at 300K and 1 standard atmosphere with Berendsen thermostat. MD simulations were conducted for a total of 50 ns and system coordinates were saved every 1 ps.

Trajectory analysis

The trajectories acquired after MD simulation were examined using the Gromacs. The root mean square deviation (RMSD) of the structure was computed with gmx rms to assess the convergence of simulation and stability of the protein. The root mean square fluctuation (RMSF) of residue was computed with gmx rmsf to determine residue flexibility. The gyration radius of the structure was calculated with gmx gyrate to determine its stability. The number of hydrogen bonds bound by small molecules to the protein during the simulation was calculated using gmx hbond. MMPBSA was utilised to compute total binding free energy during the binding of simulated small molecules to proteins, that is, Binding (molecular mechanics (MM) + Poisson Boltzmann (PB) + surface area (SA)). The Bio3D platform in R was used to plot the cross-correlation analysis between protein and residues during MD simulations, with positive values indicating that the residues moved in the same direction and negative values indicating that they moved in the opposite direction.

Results

Active ingredient and target screening results

Pruritus ani lotion combined with Huajiao-Gancao-Bingpian oil contains a total of 15 Chinese herbal medicines, 12 of which (Cortex Phellodendri, Radix Baibu, Borneol, Radix Angelicae Sinensis, Kochia scoparia, Radix Glycyrrhizae, Pericarpium Zanthoxyli Bungeani, Cortex Phellodendri, Radix Sophorae Flavescentis, Portulaca oleracea, Cnidium monnieri, and Clematis chinensis) are included in TCMSP (https://tcmsp-e.com/). A total of 241 active pharmaceutical ingredients of this formula were obtained by screening. Subsequently, targets of active ingredients were collected, yielding 186 active pharmaceutical ingredients and 283 corresponding targets after removing repeated ones (Supplementary Table S1).

PPI network construction and RWR analysis

Genes linked to pruritus ani were searched on GeneCards (Supplementary Table S2), and the top 100 genes ranked by relevance score were chosen as genes of interest. The union set of 283 target genes and these 100 disease-associated genes (Supplementary Table S3) was mapped to the network using a STRING database. A PPI network was constructed with interaction relationship pairs with confidence scores ≥ 0.7, resulting in 368 nodes and 2794 edges in the PPI network (Figure 1 A). The intersection of target genes and disease-associated genes (Figure 1 B) was selected. With a total of 15 genes as seeds (Supplementary Table S4), the PPI network was analysed by RWR, and genes with the top 50 affinity coefficient (Supplementary Table S5) were selected to generate a network of interaction among formula-active ingredient-targets (Figure 1 C).

Enrichment analyses

To investigate the functions and pathways of genes associated with pruritus ani lotion combined with Huajiao-Gancao-Bingpian Oil treatment, we selected genes with the top 50 affinity coefficients for GO and KEGG analyses. GO enrichment results indicated that genes were mainly associated with cytokine-mediated signalling pathway and cellular response to cytokine stimulus function (Figure 2 A). KEGG enrichment results showed that genes were primarily involved in the IL-17 signalling pathway, TNF signalling pathway, pathways in cancer, AGE-RAGE signalling pathway in diabetic complications, and lipid and atherosclerosis (Figure 2 B). The TNF pathway may bear some relationship with both acute and chronic pruritus [8]. Overall, these functions and signalling pathway enrichments are closely linked to cytokines.

Molecular docking

Statistical analysis of topological properties (degree) of the interaction network showed that epidermal growth factor receptor (EGFR) (Degree value: 58) and Signal Transducer and Activator of Transcription 3 (STAT3) (Degree value: 78) were in much more central positions in the interaction network of the top 50 genes (Figure 3 A). Compared with the other proteins ranked higher than EGFR and STAT3 in degree, they have a suitable pocket structure as receptor proteins. Besides, two drug molecules in the formula were found to target EGFR. Reportedly, the EGFR pathway is involved in inflammatory responses in the skin [9]. Therefore, active ingredients of the formula may directly target EGFR, affecting the conduction of EGFR, which in turn alters the status of the EGFR pathway and thus improves pruritus. According to the interaction network of drugs and genes, we found that the active ingredients targeting the EGFR gene were quercetin (MOL000098) and luteolin (MOL000356). The structure of EGFR was selected as PDB ID: 1m17, chain A, and pocket prediction was performed with quercetin and luteolin respectively, to obtain prediction results presented in Table 1. The appropriate pocket for molecular dock-

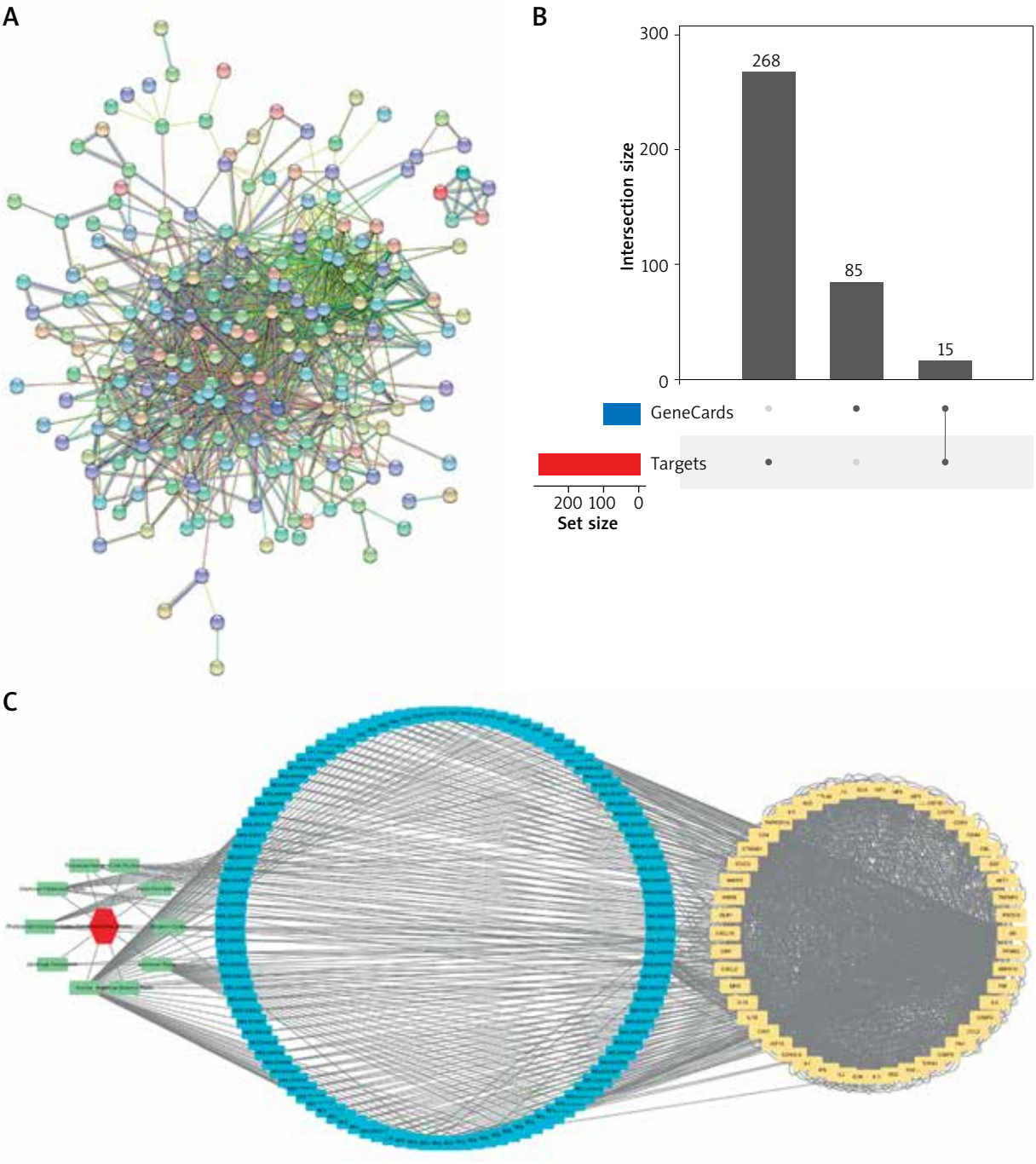

Figure 1. Formula-active component-targets interaction network of pruritus ani lotion combined with Huajiao-Gancao-Bingpian treatment. **A** – PPI network of drug target genes and pruritus ani-related genes; **B** – Intersection of target genes and pruritus ani-related genes; **C** – Interaction network of genes with the top 50 affinity coefficient and drug ingredients, with red hexagons indicating the prescription, green representing 10 herbs, blue representing 112 active substances associated with the top 50 genes, and yellow representing the top 50 genes

ing was selected from the prediction result, and docking results were depicted in Table 2. According to the affinity score of molecular docking, mode 1 binding of EGFR and quercetin had the lowest affinity score (–9 kcal/mol), which indicated a tighter bond between EGFR and small molecule quercetin. Therefore, the EGFR-quercetin complex was selected for further MD simulation. As shown in Figures 3 B and C, quercetin binds to residues around the EGFR pocket, where it forms a hydrogen bond interaction with residues Lys721 (A), Leu764 (A), Ala719 (A), Thr830

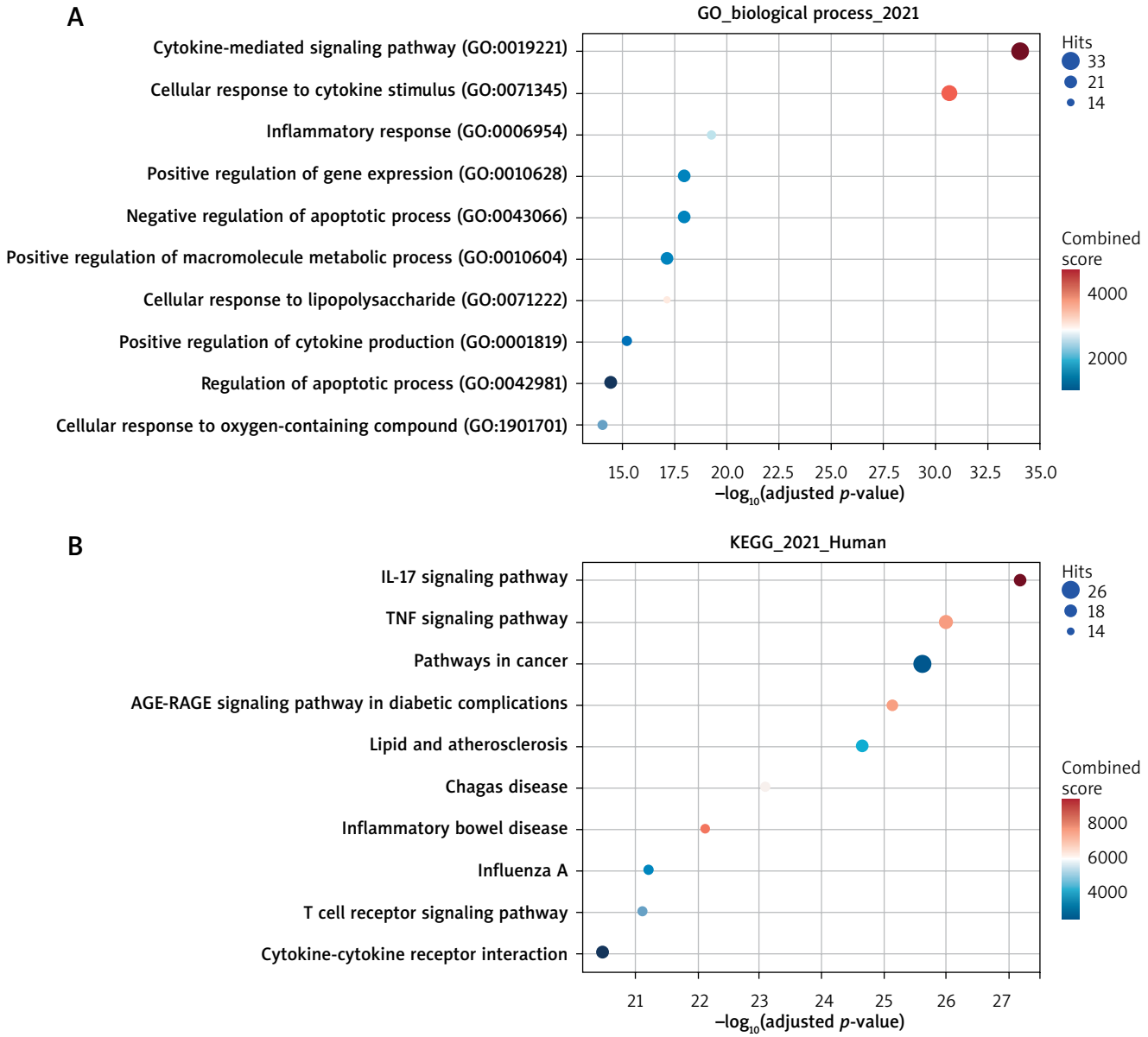

Figure 2. Enrichment analysis of the top 50 genes. **A** – GO enrichment analysis results; **B** – KEGG enrichment analysis results

(A), and Cys773 (A) of EGFR and hydrophobic interaction with residues Thr766 (A), Met742 (A), Asp831 (A), Ile720 (A), Val702 (A), Leu820 (A), and Gly772 (A).

According to one of the reports, STAT3 encourages the onset of atopic dermatitis (AD). The STAT6/STAT3 axis can be inhibited to reduce AD symptoms [10]. In a mouse model, Diospyros lotus leaf extract and myricetin inhibit STAT3 expression and improve the scratching behaviour of mice [11]. One active ingredient in the drug-gene interaction network targets STAT3, that is licochalcone A, a small molecule numbered MOL000497. Therefore, molecular docking was performed for the target protein STAT3 and its corresponding active ingredients. The selected structure of EGFR was PDB ID: P40763, chain A. Pocket prediction was performed on the structure, and prediction results are presented in Table 3. The appropriate pocket was chosen from the prediction result. Pocket 0 was chosen for molecular docking, and results are displayed in Table 4. According to the affinity of molecular docking, a lower negative value represents a closer binding of protein and small molecule. Mode 2 binding of STAT3 and licochalcone A had the lowest affinity score (–6.8 kcal/mol), so the complex of this model was selected for the next MD simulation. The binding of STAT3 to residues surrounding the licochalcone A pocket is shown in Figures 3 D and E. Licochalcone A forms hydrogen bond

Table 1. Pocket prediction results for EGFR structures

Name	Volume	Enclosure	Surface	Depth	Surf/vol	DrugScore
P_0	529.08	0.26	784.65	14.02	1.483046042	0.71883
P_1	208.33	0.09	279.02	10.52	1.339317429	0.411329
P_2	201.32	0.15	404.53	9.71	2.009388039	0.343041
P_3	196.19	0.23	439.64	9.81	2.240888934	0.36695
P_4	173.78	0.16	326.35	8.9	1.877949131	0.310828
P_5	168.17	0.15	341	8.55	2.027710055	0.277504
P_6	117.38	0.3	259.4	7.04	2.20991651	0.199908
P_7	108.69	0.08	347.17	8.95	3.194130095	0.245195
P_8	104.3	0	204.43	9.1	1.960019175	0.245489

Table 2. Molecular docking results of EGFR

Mode	Affinity [kJ/mol]	Molecule	Protein	Molecule name
1	–9	MOL000098	EGFR	Quercetin
1	–8.9	MOL000006	EGFR	Luteolin
2	–8.8	MOL000006	EGFR	Luteolin
2	–8.8	MOL000098	EGFR	Quercetin
3	–8.4	MOL000006	EGFR	Luteolin
4	–8.4	MOL000006	EGFR	Luteolin
5	–8.4	MOL000006	EGFR	Luteolin
3	–8.4	MOL000098	EGFR	Quercetin
4	–8.2	MOL000098	EGFR	Quercetin
5	–8.2	MOL000098	EGFR	Quercetin
6	–8.1	MOL000006	EGFR	Luteolin
7	–7.8	MOL000006	EGFR	Luteolin
8	–7.7	MOL000006	EGFR	Luteolin
9	–7.7	MOL000006	EGFR	Luteolin
7	–7.7	MOL000098	EGFR	Quercetin
8	–7.7	MOL000098	EGFR	Quercetin
9	–7.5	MOL000098	EGFR	Quercetin

interaction with STAT3 residue ARG262, and forms hydrophobic interaction with PRO255, HE249ARG246, ASP242, GLN141, VAL136, THR138, PRO132, and THR133.

MD simulation

Analysis of the MD simulation results was conducted based on trajectory files and energy files. RMSD (Figure 4 A), RMSF (Figure 4 B), gyration radius (Figure 4 C), and the number of hydrogen bonds of ligands and proteins during the simulation of EGFR and quercetin (Figure 4 D) were calculated. In addition, the same simulation process was carried out between STAT3 and licochalcone A (Figures 4 E–H). As per RMSD curves displayed in Figures 4 A and E, the restriction of the complex was slowly released from the starting position during simulation for 50 ns, and RMSD gradually increased and remained stable for 25–50 ns. It indicated that the conformation of protein did not change significantly after two molecules were combined, and the binding of the two was relatively stable. RMSF analysis of EGFR residues (Figure 4 B) presented that regions with larger RMSF values like residues 725 and 674 had greater residue flexibility. Besides, the secondary structures of residues 725 and 674 were loops, indicating even greater flexibility. The RMSF analysis of STAT3 residues presented that some regions of the structure, such as residues 754 and 72, had larger RMSF values (Figure 4 F), with greater residue flexibility. From the structural point of view, the secondary structure of the two regions was loop, so the flexibility was greater. The gyration radius plot revealed that the system was initially

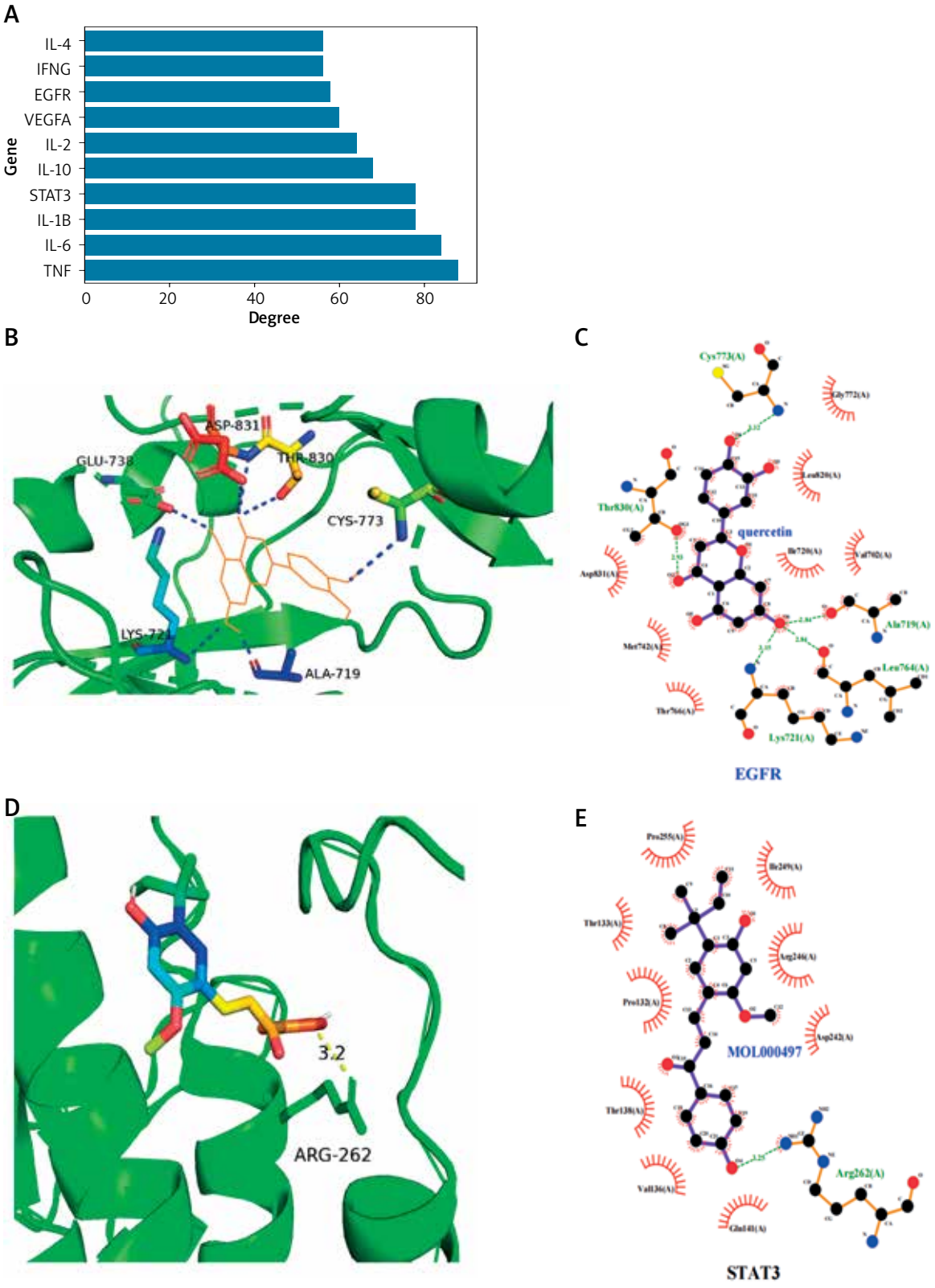

Figure 3. Molecular docking simulation analysis. **A** – Core (degree) value statistics in the interaction network, with abscissa indicating degree value and ordinate indicating the node gene; **B** – 3D plot of EGFR binding pattern to quercetin; **C** – 2D plot of EGFR binding pattern to quercetin; **D** – 3D plot of STAT3 binding pattern to licochalcone A; **E** – 2D plot of STAT3 binding pattern to licochalcone A

Table 3. Pocket prediction results for STAT3 structures

Name	Volume	Enclosure	Surface	Depth	Surf/vol	DrugScore
P_0	936.94	0.23	943.19	25.68	1.006670651	0.831709
P_1	664.3	0.18	844	19.01	1.270510312	0.786157
P_2	549.2	0.18	630.33	14.52	1.147723962	0.735764
P_3	502.45	0.1	874.51	17.3	1.740491591	0.743505
P_4	456.09	0.23	682.68	15.17	1.49680984	0.656298
P_5	443.13	0.24	605.35	16.21	1.366077675	0.684111
P_6	425.45	0.21	578.42	16.52	1.359548713	0.721061
P_7	397.17	0	490.42	14.97	1.234786112	0.649604
P_8	397.17	0.17	456.51	17.1	1.149407055	0.730683

Table 4. Molecular docking results of STAT3

Mode	Affinity [kJ/mol]	Molecule	Protein	Molecule_name
2	–6.8	MOL000497	STAT3	licochalcone A
1	–6.8	MOL000497	STAT3	licochalcone A
3	–6.4	MOL000497	STAT3	licochalcone A
4	–6.4	MOL000497	STAT3	licochalcone A
6	–6.3	MOL000497	STAT3	licochalcone A
5	–6.3	MOL000497	STAT3	licochalcone A
7	–6.2	MOL000497	STAT3	licochalcone A
9	–6.1	MOL000497	STAT3	licochalcone A
8	–6.1	MOL000497	STAT3	licochalcone A
10	–6.1	MOL000497	STAT3	licochalcone A

in a less stable condition, but as the simulation process advanced, the protein structure tended to be tight and stable, which was consistent with RMSD, demonstrating that binding the small molecule had no effect on the protein stability (Figures 4 C, G). The number of hydrogen bonds bound to EGFR by quercetin was 4, sometimes 5, for most of the 50 ns simulation (Figure 4 D), indicating that quercetin binding to EGFR was relatively stable throughout the simulated movement. In addition, during 50 ns simulation, the average number of hydrogen bonds between the molecule and STAT3 was 0.4706, indicating that the binding between the molecule and STAT3 was relatively stable during the whole simulation process (Figure 4 H).

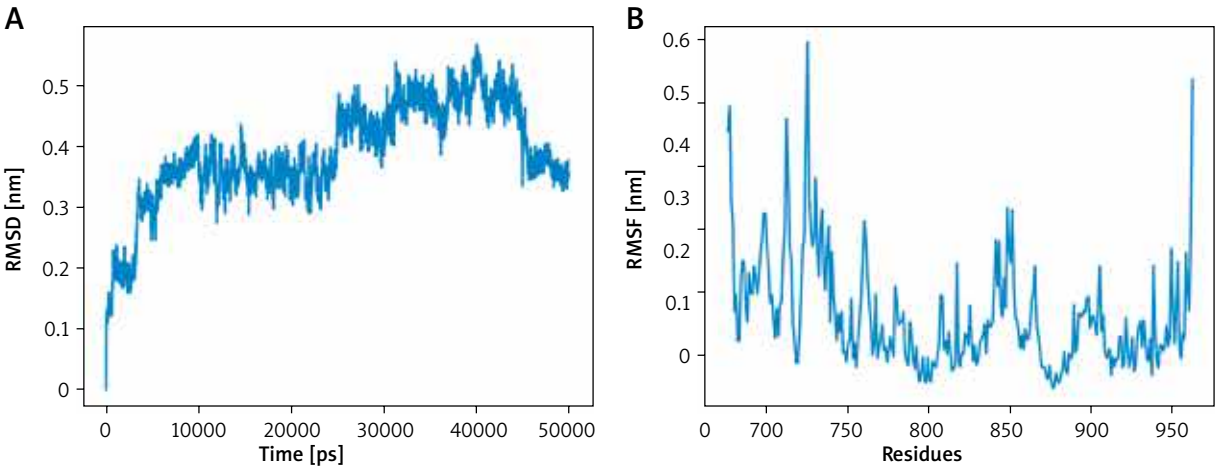

Figure 4. MD simulation analysis results. **A**–**D** – EGFR and quercetin. **A** – RMSD plot of protein backbone atoms; **B** – RMSF plot of protein residues

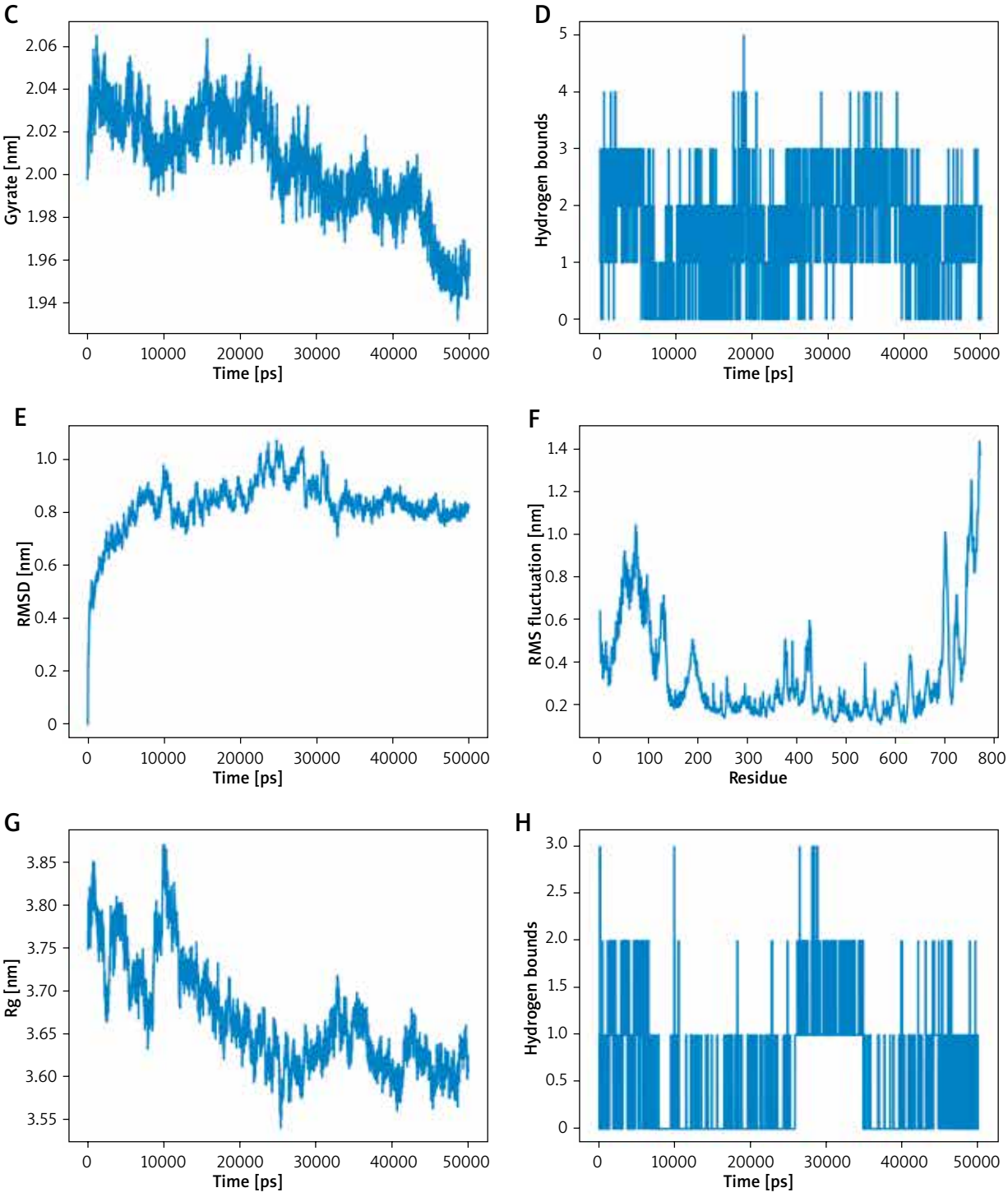

Figure 4. Cont. **A**–**D** – EGFR and quercetin. **C** – Graph of the gyration radius of the protein. **D** – Plot of the number of hydrogen bonds between quercetin and EGFR during the process; **E**–**H** – STAT3 and licochalcone A. **E** – RMSD plot of protein backbone atoms; **F** – RMSF plot of protein residues; **G** – Graph of the gyration radius of the protein; **H** – Plot of the number of hydrogen bonds between licochalcone A and STAT3 during the process

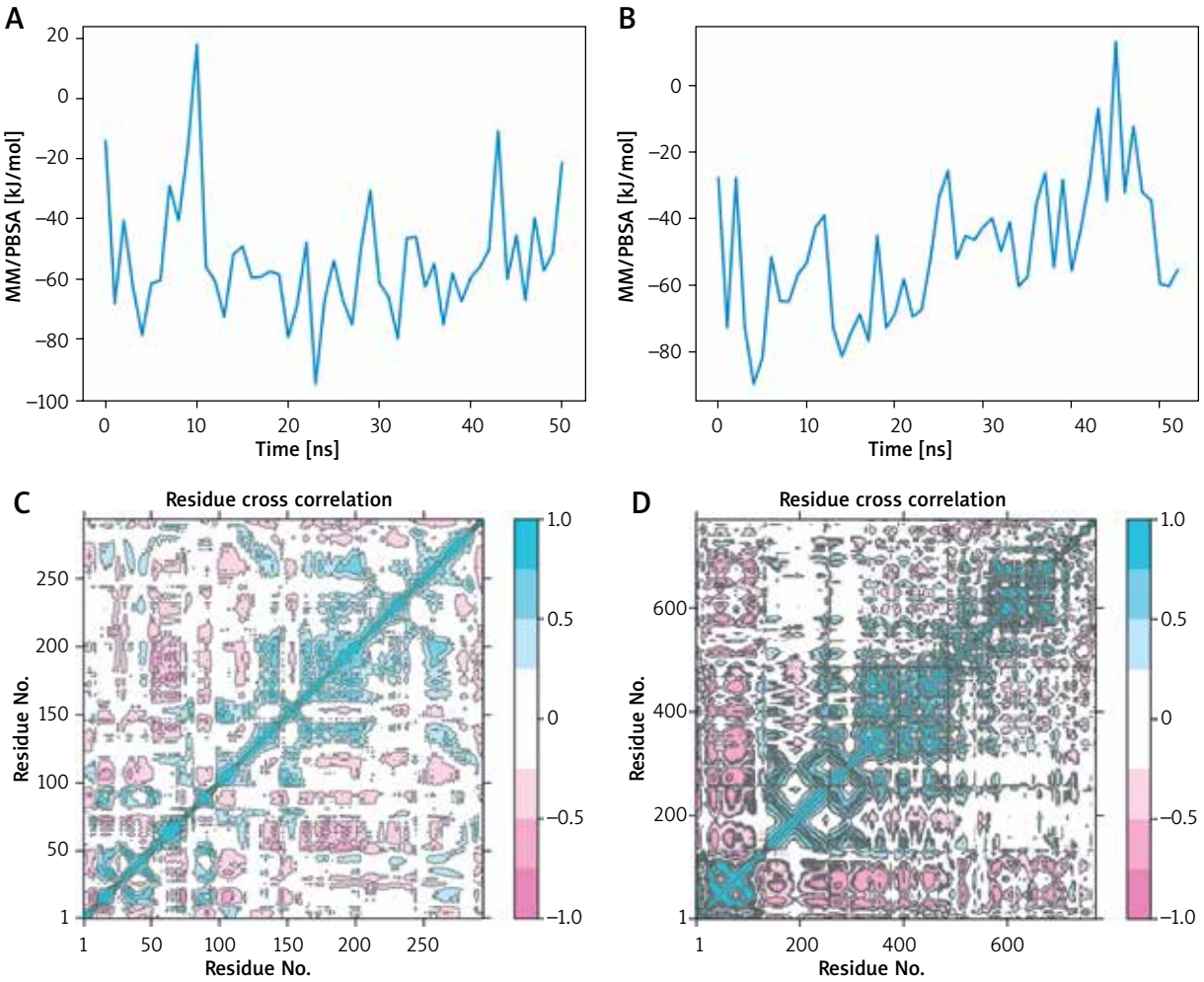

Figure 5. Binding free energy during binding. **A** – Binding free energy of quercetin to EGFR calculated by MM/PBSA; **B** – Binding free energy of licochalcone A to STAT3 calculated by MM/PBSA; **C** – Residue cross-correlation during the MD simulation process of quercetin binding to EGFR; **D** – Residue cross-correlation during the MD simulation process of licochalcone A binding to STAT3

Binding free energy calculation

MD simulation of the total binding free energy of small molecules during protein binding displayed that total free binding energy was below zero most of the time, suggesting that the binding of this molecule tended to be stable (Figures 5 A, B). The total binding free energy of EGFR and quercetin reached the mean value of –53.853 (Figure 5 A), and the total binding free energy of STAT3 and licochalcone A reached mean value of –49.73 (Figure 5 B). Following that, the findings of an analysis of the cross-correlation between protein residues during MD simulation showed that there was a correlation between residues (Figures 5 C, D).

Discussion

Currently, medication therapy, injectable therapy, and surgical treatment are the major forms of treatment for pruritus ani, a prevalent local pruritus that adversely affects patients. However, the prognosis for people with pruritus ani is still unsatisfactory based on current available therapies. Therefore, the need for medications to treat pruritus ani is urgent and has emerged as a significant scientific issue. The external treatment of pruritus ani benefits from the combination therapy [4, 12]. In this work, network pharmacology and MD were utilised to verify the efficacy of the therapy and reveal the molecular mechanisms involved.

According to the analysis of the top 50 genes interaction network, we found that EGFR, the target gene of active ingredients in pruritus ani lotion combined with Huajiao-Gancao-Bingpian oil treatment, was in the core position in the network. This finding indicated that EGFR was an extremely important target in this prescription. EGFR induces cell differentiation and proliferation of epidermal growth factor. Since cell proliferation often occurs

in epidermal epithelial tissues, lesions in these tissues may be connected to EGFR expression levels [13]. The EGFR pathway is essential for epidermal keratinocytes. EGFR inhibitors (EGFRi) targeting carcinomas can directly affect keratinocyte growth and barrier function, causing cutaneous adverse drug reactions (CADRs) such as skin inflammation, infection, itching, and dryness [13]. EGFR directly targeted by pruritus ani lotion combined with Huajiao-Gancao-Bingpian oil treatment may be a key target in the therapy of pruritus ani.

This study suggested that active molecules luteolin and quercetin targeting EGFR may be the key players in pruritus ani treatment. Natural flavonoid luteolin is antioxidant, antibacterial, anti-inflammatory, chemopreventive, anti-allergic, and anti-tumour. It has the ability to prevent or even reverse skin conditions like psoriasis, contact dermatitis, atopic dermatitis, photoaging, skin aging, and skin cancer [14]. Quercetin, a flavanol compound, is widely regarded as an all-natural, non-toxic chemopreventive agent with extraordinary antioxidant, anti-inflammatory, and anticancer properties [15]. Quercetin can target specific molecular signalling, including p53, EGFR, VEGF, STAT, PI3K/Akt, and NF-κB pathways, so as to regulate oxidative stress, tumour necrosis factor, cell cycle, proliferation, apoptosis, tumour metastasis, angiogenesis, and other tumour processes [15]. Quercetin has anti-inflammatory activity via repression of inflammatory cytokines and enzymes, as applied in the treatment of atopic dermatitis [16, 17]. In addition, *in vivo /vitro* experiments and network pharmacology have shown that Qiyin Sanliang decoction can effectively treat EGFRi-related CARD with the core active ingredients being luteolin and quercetin, which may be mediated by PTGS2, CCL2, and MMP9 in IL-17 and TNF signalling pathways [17]. Therefore, quercetin and luteolin, which target EGFR, have a positive impact on skin inflammation and may be crucial in the treatment of pruritus ani when combined with Huajiao-Gancao-Bingpian oil.

The fact that licochalcone A was stably bound to STAT3 was another crucial discovery of this research. Licochalcone A is an important flavonoid [18], which was found to have anti-inflammatory activity [19]. Licochalcone A (25–50 mg/kg) can reduce inflammation in mice with arthritis by inhibiting the secretion of proinflammatory cytokines and up-regulation of antioxidant enzyme expression through Keap1-Nrf2 signalling pathway [20]. Licochalcone A also significantly inhibited IL-2 production and secretion induced by anti-CD3 and anti-CD1 antibodies *in vivo* by inhibiting potassium (K) channels [21]. These data suggest that licochalcone A may offer an effective therapeutic avenue for inflammation-associated diseases. Our analysis found that licochalcone A could target STAT3. STAT3 is essential for transferring signals from extracellular stimuli to normal cell nuclei [22]. Lu *et al.* [23] found that inhibition of STAT3 phosphorylation could improve psoriatic skin inflammation. Moreover, STAT3 can maintain the integrity of the skin barrier by regulating the expression of SPINK5 and KLK5 in keratinocytes [24]. Thus, the targeted binding of STAT3 by licochalcone A may be crucial to the molecular mechanism of the treatment of pruritus ani.

However, as this study only looked through public databases and bioinformatics analysis was mostly used to predict and analyse the mechanism of pruritus ani lotion mixed with Huajiao-Gancao-Bingpian oil, the result we came to may be somewhat constrained. Still, more clinical and experimental data are needed for validation. In addition, the association of downstream pathways of the target genes EGFR and STAT3 with pruritus ani has not been fully investigated. We examined the relationship between target genes EGFR and STAT3 and key active molecules, luteolin, quercetin, and licochalcone A through network pharmacology and MD. The molecular basis for the external therapy of pruritus ani using pruritus ani lotion and Huajiao-Gancao-Bingpian oil was uncovered, offering theoretical backing for the clinical management and the development of novel drugs for pruritus ani.

Acknowledgments

Wenkuo Deng and Minghong Fu contributed equally.

Funding sources

None.

Conflict of interest

The authors declare no conflict of interest.

References

1. Nasseri YY, Osborne MC. Pruritus ani: diagnosis and treatment. Gastroenterol Clin North Am 2013; 42: 801-13.
2. Felemovicius I, Ganz RA, Saremi M, Christopfel W. SOOTHER TRIAL: observational study of an over-the-counter ointment to heal anal itch. Front Med (Lausanne) 2022; 9: 890883.
3. MacLean J, Russell D. Pruritus ani. Aust Fam Physician 2010; 39: 366-70.
4. Bo C, Li M, Guangyao Y. Clinical observation of Shenbai decoction sitz bath in the treatment of mild to moderate simple anal pruritus. World J Integr Trad Western Med 2020; 15: 888-91.
5. Li X, Chunhua C, Xiaokang H, Min L. Clinical efficacy of smoking versus smokeless moxibustion and the role of products of mugwort somke in antipruritic effect in treating anal pruritus. Chin General Pract 2021; 24: 1120-4.
6. Fang H, Gough J. The 'dnet' approach promotes emerging research on cancer patient survival. Genome Med 2014; 6: 64.
7. Yu G, Wang LG, Han Y, He QY. clusterProfiler: an R package for comparing biological themes among gene clusters. OMICS 2012; 16: 284-7.
8. Miao X, Huang Y, Liu TT, et al. TNF-alpha/TNFR1 Signaling is required for the full expression of acute and chronic itch in

mice via peripheral and central mechanisms. Neurosci Bull 2018; 34: 42-53.
9. Chiu LY, Wu NL, Hung CF, et al. PARP-1 involves in UVB-induced inflammatory response in keratinocytes and skin injury via regulation of ROS-dependent EGFR transactivation and p38 signaling. FASEB J 2021; 35: e21393.
10. Furue M. Regulation of skin barrier function via competition between AHR axis versus IL-13/IL-4 JAK STAT6/STAT3 axis: pathogenic and therapeutic implications in atopic dermatitis. J Clin Med 2020; 9.
11. Shin JY, Cho BO, Park JH, et al. Diospyros lotus leaf extract and its main component myricitrin regulate pruritus through the inhibition of astrocyte activation. Exp Ther Med 2023; 26: 323.
12. Wang S. Clinical observation and antibacterial test of compound Kugan mixture fumigation and wet compress in the treatment of acute perianal eczema of damp-heat injection type [Master]: Anhui University of Chinese Medicine 2014.
13. Joly-Tonetti N, Ondet T, Monshouwer M, Stamatas GN. EGFR inhibitors switch keratinocytes from a proliferative to a differentiative phenotype affecting epidermal development and barrier function. BMC Cancer 2021; 21: 5.
14. Gendrisch F, Esser PR, Schempp CM, Wolfle U. Luteolin as a modulator of skin aging and inflammation. Biofactors 2021; 47: 170-80.
15. Almatroodi SA, Alsahli MA, Almatroudi A, et al. Potential therapeutic targets of quercetin, a plant flavonol, and its role in the therapy of various types of cancer through the modulation of various cell signaling pathways. Molecules 2021; 26: 1315.
16. Karuppagounder V, Arumugam S, Thandavarayan RA, et al. Molecular targets of quercetin with anti-inflammatory properties in atopic dermatitis. Drug Discov Today 2016; 21: 632-9.
17. Wang Y, Zhang Y, Ding C, et al. Exploration of the potential mechanism of Qi Yin San Liang San decoction in the treatment of EGFRI-related adverse skin reactions using network pharmacology and in vitro experiments. Front Oncol 2022; 12: 790713.
18. Simmler C, Lankin DC, Nikolić D, et al. Isolation and structural characterization of dihydrobenzofuran congeners of licochalcone A. Fitoterapia 2017; 121: 6-15.
19. Li MT, Xie L, Jiang HM, et al. Role of licochalcone A in potential pharmacological therapy: a review. Front Pharmacol 2022; 13: 878776.
20. Su X, Li T, Liu Z, et al. Licochalcone A activates Keap1-Nrf2 signaling to suppress arthritis via phosphorylation of p62 at serine 349. Free Radical Biol Med 2018; 115: 471-83.
21. Phan HTL, Kim HJ, Jo S, et al. Anti-inflammatory effect of licochalcone A via regulation of ORAI1 and K(+) channels in T-lymphocytes. Int J Mol Sci 2021; 22: 10847.
22. Levy DE, Darnell JE Jr. Stats: transcriptional control and biological impact. Nat Rev Mol Cell Biol 2002; 3: 651-62.
23. Lu H, Gong H, Du J, et al. Piperine ameliorates psoriatic skin inflammation by inhibiting the phosphorylation of STAT3. Int Immunopharmacol 2023; 119: 110221.
24. Kim J, Kim MG, Jeong SH, et al. STAT3 maintains skin barrier integrity by modulating SPINK5 and KLK5 expression in keratinocytes. Exp Dermatol 2022; 31: 223-32.